# Interleukin-15 regulates proliferation and self-renewal of adult neural stem cells

Diego Gómez-Nicola[a,b], Beatriz Valle-Argos[a], Noemí Pallas-Bazarra[a], and Manuel Nieto-Sampedro[a,b]

[a]Functional and Systems Neurobiology Department, Cajal Institute (CSIC), Madrid, Spain; [b]Experimental Neurology Unit, National Hospital of Paraplegics (SESCAM), Toledo, Spain

**ABSTRACT** **The impact of inflammation is crucial for the regulation of the biology of neural stem cells (NSCs). Interleukin-15 (IL-15) appears as a likely candidate for regulating neurogenesis, based on its well-known mitogenic properties. We show here that NSCs of the subventricular zone (SVZ) express IL-15, which regulates NSC proliferation, as evidenced by the study of IL-15−/− mice and the effects of acute IL-15 administration, coupled to 5-bromo-2′-deoxyuridine/5-ethynyl-2′-deoxyuridine dual-pulse labeling. Moreover, IL-15 regulates NSC differentiation, its deficiency leading to an impaired generation of neuroblasts in the SVZ–rostral migratory stream axis, recoverable through the action of exogenous IL-15. IL-15 expressed in cultured NSCs is linked to self-renewal, proliferation, and differentiation. IL-15−/− NSCs presented deficient proliferation and self-renewal, as evidenced in proliferation and colony-forming assays and the analysis of cell cycle–regulatory proteins. Moreover, IL-15–deficient NSCs were more prone to differentiate than wild-type NSCs, not affecting the cell population balance. Lack of IL-15 led to a defective activation of the JAK/STAT and ERK pathways, key for the regulation of proliferation and differentiation of NSCs. The results show that IL-15 is a key regulator of neurogenesis in the adult and is essential to understanding diseases with an inflammatory component.**

**Monitoring Editor**
Carl-Henrik Heldin
Ludwig Institute for Cancer Research

Received: Jan 20, 2011
Revised: Mar 16, 2011
Accepted: Apr 8, 2011

## INTRODUCTION

Adult neurogenesis is a cell-replacing process occurring continuously in the subventricular zone (SVZ) of the lateral ventricle and the subgranular zone of the hippocampal dentate gyrus (Doetsch *et al.*, 1999; Alvarez-Buylla *et al.*, 2001). Signals coming from the cellular environment control the intrinsic proliferation and differentiation programs of neural stem cells (NSCs); these inflammatory signals are key regulators during neuropathological states (Monje *et al.*, 2003; Carpentier and Palmer, 2009). The balance between proinflammatory and anti-inflammatory molecules regulates neurogenesis (Ekdahl *et al.*, 2009). Cytokines such as interleukin (IL)-1β, -4, or -6, interferon-γ, and tumor necrosis factor (TNF)-α have been proposed to mediate direct effects on the neurogenic niches, regulating NSC proliferation and differentiation through mitogen-activated protein kinase (MAPK) or Janus kinase/signal transducers and activators of transcription (JAK/STAT) pathways, determining the final outcome of adult neurogenesis (Vallieres *et al.*, 2002; Monje *et al.*, 2003; Butovsky *et al.*, 2006; Koo and Duman, 2008; Samuels *et al.*, 2008; Bauer, 2009; Li *et al.*, 2010).

Interleukin-15 is a pleiotropic proinflammatory cytokine with relevant actions in both the immune and the nervous systems (Budagian *et al.*, 2006). In the CNS IL-15 is expressed in vivo in both astrocytes and some neuronal populations, to be found in microglial cells in vitro and after an inflammatory stimulus (Hanisch *et al.*, 1997; Gomez-Nicola *et al.*, 2008a). It is upregulated after injury, assuming a leading role during the development of neuroinflammation and microglial activation (Huang *et al.*, 2007; Gomez-Nicola *et al.*, 2008a, 2008b, 2010b, 2010c). IL-15 also influences anxiety- or depression-related behavior and has been recently suggested to regulate hippocampal-dependent memory (He *et al.*, 2010; Wu *et al.*, 2010, 2011). Moreover, increasing evidence suggests a role of IL-15 as a regulator of neurogenesis. IL-2, a cytokine with high homology with

This article was published online ahead of print in MBoC in Press (http://www.molbiolcell.org/cgi/doi/10.1091/mbc.E11-01-0053) on April 20, 2011.

Address correspondence to: Diego Gómez-Nicola (dgomeznicola@gmail.com).

Abbreviations used: BrDU, 5-bromo-2′deoxyuridine; DCX, doublecortin; EdU, 5-ethynyl-2′-deoxyuridine; GFAP, glial fibrillary acidic protein; IL-15, interleukin 15; JAK/STAT, Janus kinase/signal transducer and activator of transcription; MAPK, mitogen activated protein kinase; NSCs, neural stem cells; RMS, rostral migratory stream; SVZ, subventricular zone.

IL-15 in both structure and functions, was shown to have a negative effect on adult neurogenesis (Beck *et al.*, 2005). Recently the alpha subunit of the IL-15 receptor (IL-15Rα) was reported to regulate neuronal differentiation of cultured NSCs (Huang *et al.*, 2009). Of greater interest, recent work reported a decrease in olfactory bulb epithelium neurogenesis in IL-15Rα knockout mice (Umehara *et al.*, 2009), pointing to a role of the IL-15 system in regulating adult neural populations. Furthermore, IL-15 has been described as a regulator of progenitor cell differentiation to NK cells (Fehniger and Caligiuri, 2001; Budagian *et al.*, 2006; Benson *et al.*, 2009) and as a mitogenic signal for immune cells, directly activating the MAPK and JAK/STAT signaling pathways (Gadina *et al.*, 2000; Giron-Michel *et al.*, 2003; Budagian *et al.*, 2006; de Totero *et al.*, 2008; Gomez-Nicola *et al.*, 2010c). These features make IL-15 a suitable candidate for the regulation of NSC self-renewal, proliferation, or differentiation, with increased relevance in the context of the neuroimmune component of neuropathology.

In this work we provide evidence, using both in vivo and in vitro experimental models, for an important regulatory role of IL-15 in adult neurogenesis, controlling self-renewal, proliferation, and differentiation of neural stem cells and serving as a key link for in the neuroinflammatory control of neurogenesis.

## RESULTS

### IL-15 is expressed in the subventricular zone and the rostral migratory stream

Immunohistochemical analysis of IL-15 expression showed immunopositive labeling in both the subventricular zone (SVZ) and the rostral migratory stream (RMS) (Figure 1, A, F, and G). Within the SVZ IL-15 was expressed in glial fibrillary acidic protein (GFAP)-positive NSCs, as shown by immunofluorescent colocalization (Figure 1, B, C, and C*). Moreover, IL-15Rα was found to be expressed in nestin-positive cells of the SVZ (Figure 1, D and E). In the RMS, the expression of IL-15 was found in the migratory mass, colocalizing with doublecortin-positive neuroblasts (DCX+; Figure 1, I, K, and K*), as shown by double immunofluorescence. IL-15 expression was not found in GFAP-positive astrocytes of the RMS (Figure 1, H, J, and J*).

### Neurogenesis is decreased in IL-15 knockout mice

To investigate the effect of IL-15 on adult neurogenesis, we studied the neurogenic potential of IL-15 knockout mice (IL-15−/−). Adult mice received intraperitoneal injections of 5-bromo-2′-deoxyuridine (BrDU) for 2 d to further evaluate its incorporation in the neurogenic niche by immunohistochemical means (Figure 2). IL-15−/− mice showed significant reduction in the number of BrDU+ nuclei within the SVZ when compared with their wild-type (WT) littermates (Figure 2, A, B, and E). This reduction correlated with the expression of DCX, with IL-15−/− mice presenting a significant decrease of the DCX+ area when compared with their WT littermates (Figure 2, G, H, and K). Moreover, the number of neuroblasts in the RMS was also significantly reduced in the IL-15−/− mice, presenting both fewer BrDU+ cells (Figure 2, C, D and F) and more reduced DCX+ area (Figure 2, I, J, and L) than their WT littermates.

### IL-15 promotes proliferation of neural stem cells

Taking into account the observed loss of neurogenic potential in IL-15−/− mice, we proceeded to address the potential of IL-15 to promote neurogenesis in a gain-of-function experimental paradigm (Figure 3). The effect of the intraventricular administration of IL-15 was evaluated by sequential administration of 5-ethynyl-2′-deoxyuridine (EdU) and BrDU and immunohistochemical analysis in IL-15−/− and WT animals (Figure 3; see experimental scheme). The

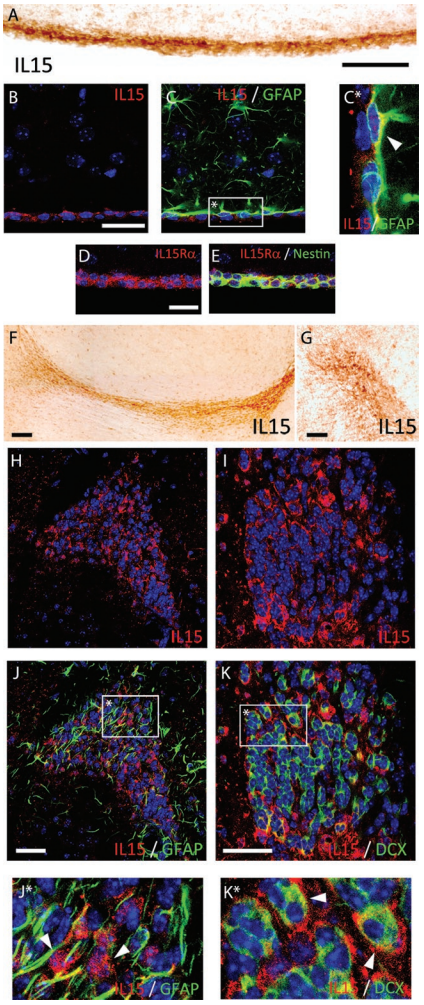


FIGURE 1: IL-15 expression in the SVZ and RMS. (A, F–G) Immunostaining of IL-15+ cells in the SVZ (A) and the RMS (F, sagittal; G; coronal). (B, C) Double immunofluorescence for IL-15 (red; B, C) and GFAP (green; C) in the SVZ. (C*) Inset: magnification of IL-15 colocalization in GFAP+ cells (white arrowhead). (D, E) Double immunofluorescence for IL-15Rα (red; D, E) and nestin (green; E) in the SVZ. (H–K) Double immunofluorescence for IL-15 (red; H, J and I, K) and GFAP (green; J) or DCX (green; K) in the RMS. (J*, K*) Inset: magnification of IL-15 colocalization in GFAP− cells (J*; white arrowhead) and DCX+ cells (K*; white arrowhead). Nuclei are stained with Hoechst (blue). Fluorescent sections are evaluated with confocal microscopy. Scale bar in A–E and G–K, 50 μm (shown in A, B, D, G, J, K); in F, 100 μm.

comparison of the pattern of incorporation of EdU in WT or IL-15−/− mice (Figure 3, A, D, N, and O) correlated with that observed previously with BrDU (Figure 2) at both the SVZ and RMS levels, supporting the observed deficit in neurogenesis of IL-15−/− mice. When recombinant IL-15 was administered intraventricularly (ICV) a rescue in the phenotype of IL-15−/− mice was observed. Thus intraventricular IL-15 caused an increase in the proliferation in the SVZ both in WT (Figure 3, G–I) and IL-15−/− (Figure 3, J–L) mice when compared with the injection of phosphate-buffered saline (PBS) (Figure 3, A–C and D–F). On considering the BrDU/EdU ratio of incorporation, a significant increase in IL-15−/− injected with IL-15 when compared with PBS was found, pointing to a recovery of the normal function (Figure 3M).

The RMS was also analyzed for the incorporation of EdU and BrDU in the proposed experimental paradigm. The administration

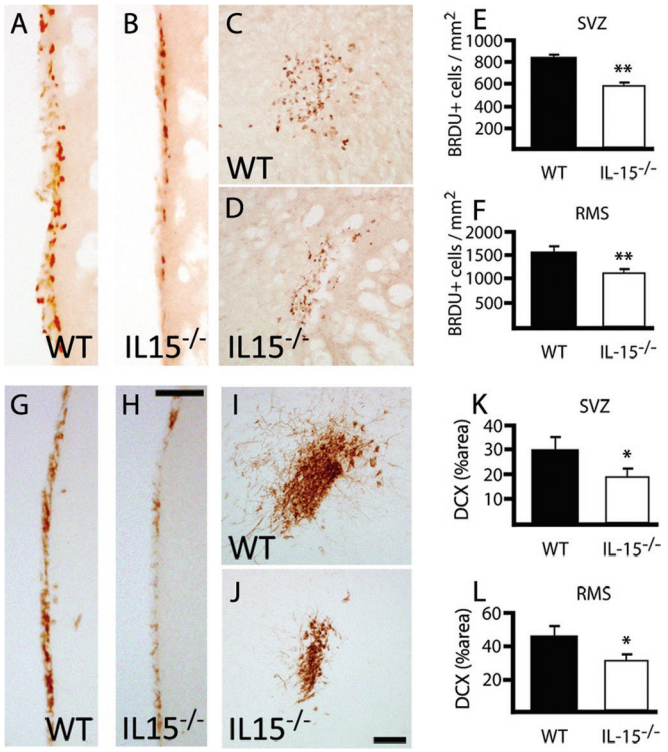


FIGURE 2: Neurogenesis is decreased in IL-15−/− mice. (A–D) Immunohistochemical analysis of the incorporation of BrDU in the SVZ (A, B) and the RMS (C, D) of WT (A, C) and IL-15−/− (B, D) mice. (E, F) Quantification of BrDU+ nuclei in the SVZ (E) and the RMS (F) of WT and IL-15−/− mice, expressed as mean ± SEM of BrDU+ nuclei/mm$^2$. (G–J) Immunohistochemical analysis of the incorporation of BrDU in the SVZ (G, H) and the RMS (I, J) of WT (G, I) and IL-15−/− (H, J) mice. (K, L) Quantification of the DCX+ area in the SVZ (K) and the RMS (L) of WT and IL-15−/− mice, expressed as mean ± SEM of percent DCX+ area. Scale bar in A–D and G–J, 50 μm. Statistical differences of WT vs. IL-15−/−: *$p < 0.05$, **$p < 0.01$. Data were analyzed with an analysis of variance (ANOVA) and a post hoc Tukey test.

of ICV IL-15 caused a recovery of the phenotype of IL-15−/− mice, as shown by the significant increase of the ratio BrDU/EdU (Figure 3, P–R). The administration of the vehicle (PBS) did not cause any change in WT or IL-15−/− mice (Figure 3, N and O), given the differences between both types of mice based on the previously described neurogenic deficiencies. Of interest, the administration of IL-15 also caused a dispersion of the RMS proliferative cells outside the margins of the stream delimited by nuclei staining in both the WT and IL-15−/− mice (Figure 3, P and Q).

We compared next the effect of the ICV injection of IL-15 on the neurogenic potential of both WT and IL-15−/− mice (Figure 4). IL-15−/− mice presented, as previously described (Figure 2), a decreased population of DCX+ cells within the SVZ (Figure 4, A and D) and the RMS (Figure 4, O and P). The administration of IL-15 caused an increase in the DCX+ population in both the WT (Figure 4, G–I) and the IL-15−/− (Figure 4, J–L) mice, with the latter recovering the WT phenotype. Quantification of the DCX+ area within the SVZ showed a significant increase on treatment with IL-15 in both the WT and IL-15−/− mice (Figure 4M). The analysis of the RMS correlated with that observed in the SVZ. ICV IL-15 caused a significant increase in the DCX+ population in both WT (Figure 4, O and Q) and IL-15−/− mice (Figure 4, P and R), leading to a recovery of the WT phenotype in the latter (Figure 4S).

The GFAP+ population was concomitantly affected by the injection of IL-15 at both the SVZ and RMS levels. ICV IL-15 caused an increase in GFAP labeling, generating more reactive-like phenotypes, which were in all cases less abundant in IL-15−/− mice (Figure 4, H, K, Q, and R). The analysis of the expression of GFAP in the SVZ and the RMS showed an increase in the levels of the protein in response to the intraventricular injection of IL-15. This action was only observed in the WT mice, with IL-15−/− mice having a defective response to the IL-15 (Figure 4, N and T).

### Expression of IL-15 in neurospheres is implicated in both proliferation and differentiation

The results obtained in vivo led us to analyze the effect of IL-15 on the biology of cultured neural stem cells (neurospheres). First, we observed that IL-15 was expressed in neurospheres, being expressed by a small number of cells within the neurosphere mass (Figure 5, A and D). The IL-15-expressing cells were a subgroup of nestin-positive (Figure 5B) and DCX-positive (Figure 5E) cells, as shown by immunocytochemical colocalization (Figure 5, C and F). The expression of IL-15 mRNA was found under nonproliferating conditions (Figure 5G; CTL) but was upregulated upon proliferative stimulation with epidermal growth factor (EGF) and fibroblast growth factor (FGF), reaching its maximal expression at 24 h after the stimuli, to further decrease (Figure 5G). On the other hand, the elevated expression of IL-15 during proliferation (EGF + FGF) decreases when neurospheres are cultured under adherent and differentiation conditions (2% fetal bovine serum [FBS]), as observed after a 4- to 10-d differentiation paradigm (Figure 5H).

### IL-15 promotes self-renewal and proliferation of neural stem cells

The previously obtained results with different in vivo or in vitro experimental paradigms led us to question whether IL-15 is important for NSC proliferation and/or self-renewal. Therefore, using cultured neurospheres derived from WT or IL-15−/− mice, we analyzed the effect of exogenous IL-15 on neurosphere proliferation and self-renewal. First, WT neurospheres significantly increase their proliferation when stimulated with recombinant exogenous IL-15 under nonproliferative culture conditions (Nb + B27 supplement; Figure 6A). Second, when WT or IL-15−/− neurospheres were cultured under proliferative conditions (Nb + B27 + EGF + FGF), we observed a deficiency of IL-15−/−-derived neurospheres to reach a normal WT proliferative rate (Figure 6B). IL-15−/−-derived neurospheres showed a significant reduction in their proliferation at both 48 and 72 h after the addition of the mitogenic boost (Figure 6B).

To investigate the molecular basis for the observed decreased proliferation potential of IL-15−/− NSCs, we studied the expression of the main regulators of the cell cycle (Figure 6C). Under WT conditions, the addition of the mitogenic stimulus of EGF + FGF to the NSCs induce an up-regulation of the expression of the cyclins D1 and D3 and the cyclin-dependent kinases 4 and 6 (CDK4/6; Figure 6C). These proteins form complexes that phosphorylate the retinoblastoma protein (Rb), causing its release from the transcription factors that permit the transition from the G1 to S phases of the cell cycle (Figure 6C). The correct progression of the cell cycle permits the phosphorylation of the histone H3 during the mitosis phase (Figure 6C). In contrast, the mitogenic input cause a reduction of the expression of the cell cycle inhibitors p15, p21, and p27, which regulates the formation and activity of the cyclin/CDK complexes (Figure 6C). Investigation of the expression of these proteins in IL-15−/− neurospheres showed an alteration of the cell cycle regulation responsible for the decreased proliferation

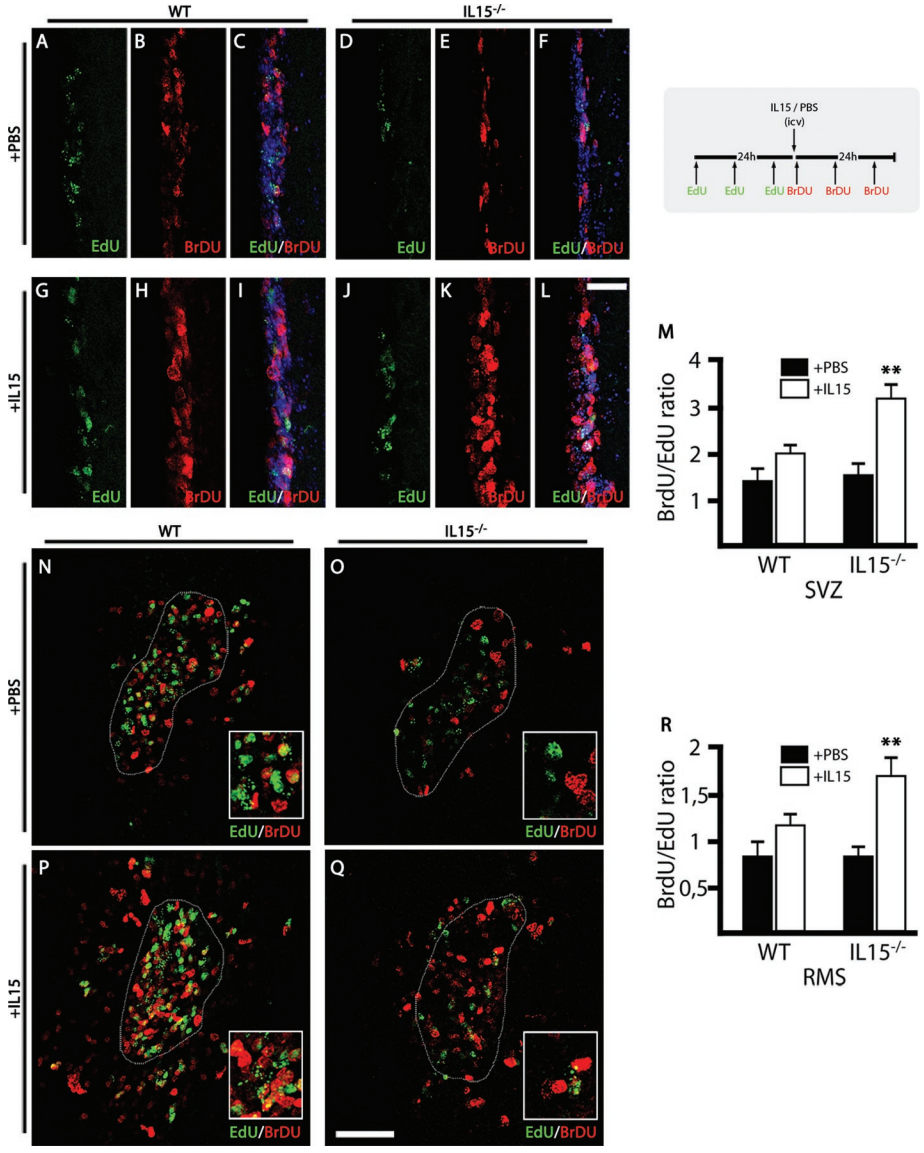


FIGURE 3: Intraventricular IL-15 increases NSC proliferation and rescues IL-15−/− phenotype. Dual-pulse (BrDU/EdU) analysis of the effect of IL-15 on NSC proliferation in WT and IL-15−/− mice (see experimental scheme at top right corner). (A–L) Double immunofluorescence for EdU (green) and BrdU (red) in the SVZ of WT (A–C, G–I) and IL-15−/− (D–F, J–L) mice after treatment with ICV PBS (A–F) or IL-15 (1 µg/5 µl; G–L). (M) Quantification of the effect of the ICV injection of PBS (black bars) or IL-15 (white bars) on the proliferative activity in the SVZ of WT or IL-15−/− mice, as mean ± SEM of BrdU/EdU+ nuclei ratio. (N–Q) Double immunofluorescence for EdU (green) and BrdU (red) in the RMS of WT (N, P) and IL-15−/− (O, P) mice after treatment with ICV PBS (N, O) or IL-15 (1 µg/5 µl; P, Q). (R) Quantification of the effect of the ICV injection of PBS (black bars) or IL-15 (white bars) on the proliferative activity in the RMS of WT or IL-15−/−mic, as mean ± SEM of BrdU/EdU+ nuclei ratio. Magnifications are shown in the low right-hand insert. Nuclei are stained with Hoechst (blue). Immunopositive nuclei counting was delimited to the RMS perimeter (dotted line), established using Hoechst staining. Fluorescent sections were evaluated with confocal microscopy. Scale bar in A–L, 20 µm (shown in L); in N–Q, 50 µm (shown in Q). Statistical differences of PBS vs. IL-15: **p < 0.01. Data were analyzed with an ANOVA and a post hoc Tukey test.

observed between 48 and 72 h. The expression of both cyclins D1/D3 and CDK4/6 do not reach the levels observed in WT NSCs (Figure 6C). In consequence, IL-15−/− NSCs presented a deficient phosphorylation of the Rb protein compared with WT NSCs (Figure 6C). In contrast, the expression of the cell cycle inhibitors p15, p21, and p27 is increased in IL-15−/− NSCs when compared with the WT NSCs (Figure 6C).

The self-renewal ability of the IL-15−/− neurospheres was also analyzed (Figure 6, D–F). NSCs from WT or IL-15−/− mice were cultured with a cloning protocol for obtaining secondary neurospheres. Primary neurospheres were dissociated and re-seeded as single cells to let them grow for 7 d under proliferative conditions. IL-15−/−-derived NSCs presented a significant reduction in the number of forming neurospheres when compared with the WT-derived NSCs at the three assayed dilution conditions (5, 50, or 500 initial cells/well; Figure 6E). Moreover, the average size of the formed neurospheres, after 7 d of cloning assay, was significantly smaller in the IL-15−/−-derived cells than in the WT cells (Figure 6, D and F).

Together, these results point to direct effect of IL-15 on the promotion of both NSC proliferation and self-renewal.

## IL-15 regulates differentiation of neural stem cells

Taking into account the observed changes in IL-15 expression in NSCs during the course of their differentiation (Figure 5), we proceeded to analyze the effect of IL-15 knockout on the NSC differentiation profile. NSCs were cultured under differentiating conditions (supplemented with 2% FBS) for 4, 7, and 10 d to further analyze the expression of neuronal, astroglial, or oligodendroglial specific markers by Western blotting and immunocytochemistry (Figure 7). First, we observed that IL-15−/− NSCs presented an accelerated and enhanced differentiation pattern when compared with WT NSCs, as deduced from the increased levels of GFAP, βIII tubulin, and myelin basic protein (MBP) (markers of astrocytes, neurons, and oligodendrocytes, respectively) at any analyzed time point (Figure 7A). On the other hand, the expression of DCX was quickly downregulated in IL-15−/− NSCs compared with WT cells (Figure 7A), indicating a more acute loss of the undifferentiated state. Specifically, we observed in IL-15−/− NSCs that both GFAP and βIII tubulin levels reach their maximum at 4 d, to be maintained for the whole course of differentiation, whereas MBP levels increased progressively with time (Figure 7A).

These results correlate with the analysis by immunocytochemistry of the cellular populations at different time points of differentiation (Figure 7B). WT NSCs progressively increase the numbers of GFAP+ astrocytes and O4+ oligodendrocytes, whereas the proportion of βIII tubulin+ neurons decreased (Figure 7B). IL-15−/− NSCs present a significantly increased population of βIII tubulin+ and GFAP+ cells when compared with WT cells (Figure 7B), with a marked reduction of the undifferentiated population at early time points.

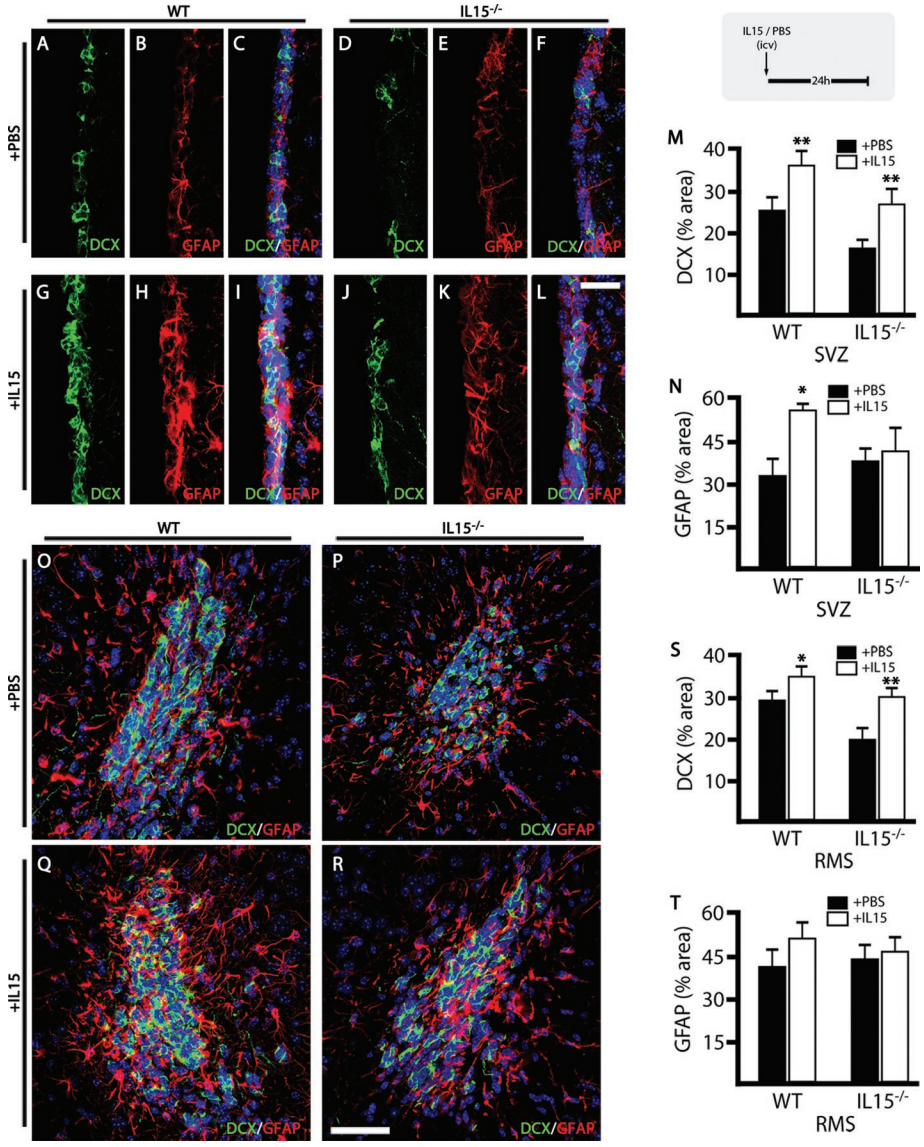


FIGURE 4: Intraventricular IL-15 increases the pool of neuroblasts and rescues IL-15−/− phenotype. Analysis of the effect of IL-15 on neurogenesis in WT and IL-15−/− mice (see experimental scheme at top right corner). (A–L) Double immunofluorescence for DCX (green) and GFAP (red) in the SVZ of WT (A–C, G–I) and IL-15−/− (D–F, J–L) mice after treatment with ICV PBS (A–F) or IL-15 (1 μg/5 μl; G–L). (M, N) Quantification of the effect of the ICV injection of PBS (black bars) or IL-15 (white bars) on the expression of DCX (M) and GFAP (N) in the SVZ of WT or IL-15−/− mice, as mean ± SEM of percent positive area. (O–R) Double immunofluorescence for DCX (green) and GFAP (red) in the RMS of WT (O, Q) and IL-15−/− (P, R) mice after treatment with ICV PBS (O, P) or IL-15 (1 μg/5 μl; Q, R). (S, T) Quantification of the effect of the ICV injection of PBS (black bars) or IL-15 (white bars) on the expression of DCX (M) and GFAP (N) in the RMS of WT or IL-15−/− mice as mean ± SEM of percent positive area. Nuclei are stained with Hoechst (blue). Fluorescent sections are evaluated with confocal microscopy. Scale bar in A–L, 20 μm (shown in L); in O–R, 50 μm (shown in R). Statistical differences of PBS vs. IL-15: *$p < 0.05$, **$p < 0.01$. Data were analyzed with an ANOVA and a post hoc Tukey test.

To summarize, the absence of IL-15 increases the overall differentiation potential of NSCs, pointing to a role of IL-15 in the maintenance of the self-renewal and undifferentiated state.

### IL-15−/− NSCs have decreased activation of the extracellular signal-regulated kinase and JAK/STAT pathways

Knowing that most of the proliferative and differentiation patterns of NSCs are regulated by the MAPK and JAK/STAT pathways, we wanted to investigate whether these pathways were differentially regulated in IL-15−/− NSCs. Using Western blotting techniques, we observed that WT NSCs showed an increased phosphorylation of extracellular signal-regulated kinase (ERK) 1 and ERK2 when stimulated with EGF and FGF, with maximal values 5 min after the stimulus (Figure 8A). IL-15−/− NSCs present a decreased activation of the ERK1/2 pathway, evidenced by a decrease in the phosphorylation of both ERK and ERK2 when compared with the WT cells (Figure 8A). The JAK/STAT pathway activation was analyzed through the phosphorylation state of STAT1, STAT3, and STAT5. On stimulation with EGF and FGF, WT NSCs present an increased phosphorylation of STAT1, STAT3, and STAT5 (Figure 8B). However, when IL-15 is knocked out, the phosphorylation degree of STAT1, STAT3, and STAT5 decreased to near-resting levels. Only residual phosphorylation was observed in either WT or IL-15−/− NSCs cultured under resting conditions (without EGF and FGF).

Moreover, the proliferative effect of IL-15 on neural stem cells observed previously (Figure 6A) reverted when either the ERK1/2 or the JAK/STAT pathway was blocked (Figure 8C). A complete repression of the mitogenic effects was only observed when both signaling pathways were simultaneously inhibited (Figure 8C), suggesting that IL-15 effects were not based on the activation of a specific pathway.

## DISCUSSION

In the present work we provide evidence for the role of IL-15 as an important regulator of adult neural stem cell self-renewal, proliferation, and differentiation. Using both in vivo and in vitro experimental paradigms of either loss or gain of function of IL-15, we observed that the cytokine maintains NSC self-renewal and promotes neurogenesis, with the reduction of IL-15 levels leading to enhanced cell differentiation. Our findings are in line with previous works that suggested a role for IL-15 in the regulation of neurogenesis. Recent work reported the expression of IL-15 and IL-15Rα in neuronal precursors of the developing olfactory epithelium (Umehara *et al.*, 2009). These authors also reported a decrease in olfactory neurons and cell proliferation in the olfactory epithelium niche in IL-15Rα knockout mice (Umehara *et al.*, 2009), supporting our proliferation-related findings in IL-15 knockout mice SVZ. Cultured postnatal NSCs present a defective proneural differentiation on treatment with IL-15 (Huang *et al.*, 2009), coinciding with our results from studying the differentiation of IL-15 knockout adult NSCs and supporting the role of the cytokine for the maintenance of NSC self-renewal. The study of IL-2 function on neurogenesis points to an

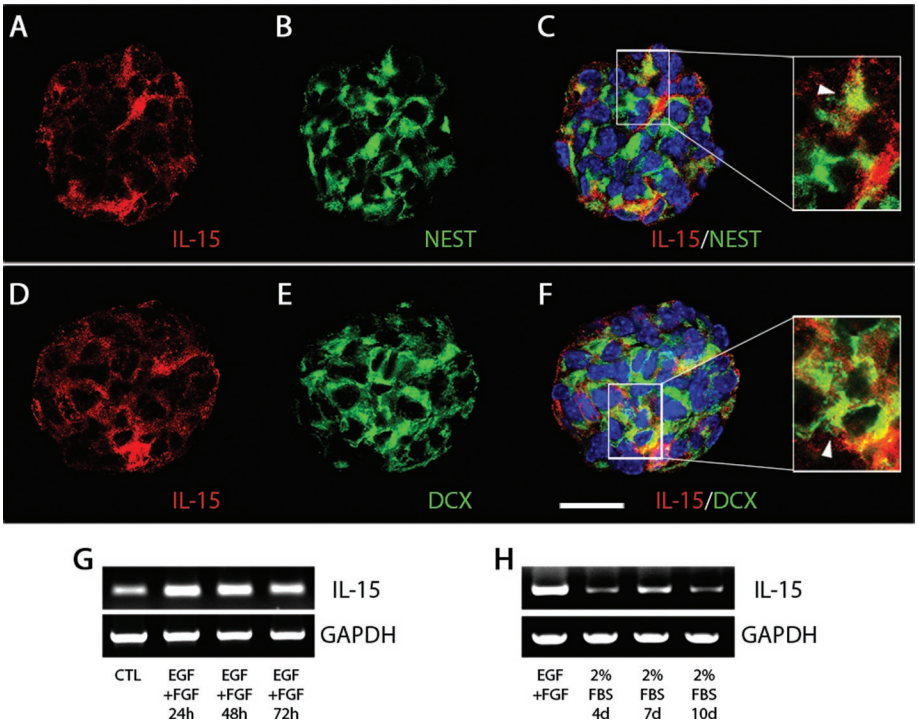


FIGURE 5: IL-15 is expressed in neurospheres during proliferation and differentiation. (A–F) Immunocytochemical analysis of the expression of IL-15 (red; A, C, D, F) in nestin-positive (green; B, C) or DCX-positive (green; E, F) cells. Magnifications are shown in the right-hand inset, indicating colocalization with white arrowheads. Nuclei are stained with Hoechst (blue). Neurospheres were evaluated with confocal microscopy. Scale bar in A–F, 20 μm (shown in F). (G) RT-PCR analysis of IL-15 mRNA expression under proliferative culture conditions (+EGF, +FGF) at 24, 48, and 72 h. Resting neurospheres (without EGF or FGF) were used as control (CTL). GAPDH expression was used as housekeeping gene. (H) RT-PCR analysis of IL-15 mRNA expression under differentiation culture conditions (+2% FBS) at 4, 7, and 10 d. Proliferative neurospheres (+EGF, +FGF) were used as control. Glyceraldehyde 3-phosphate dehydrogenase (GAPDH) expression was used as housekeeping gene.

increased hippocampal neurogenesis in IL-2 knockout mice, with a simultaneous increase of IL-15 levels (Beck *et al.*, 2005). This contrasting and complementary effect of closely related cytokines could be explained by a different use of the receptor complex, accounting for opposing functions, as previously described in other cell models (Budagian *et al.*, 2006). Thus the results obtained in our work are relevant for the understanding of the molecular control of adult neurogenesis both in normal conditions and in the neuroinflammatory context during CNS neuropathology.

During a neurodegenerative process, neurogenesis and neural stem cell differentiation are affected by the local environment. With astroglial and microglial activation as common features of these pathologies, a balance between neuroprotective and neurotoxic mediators controls neural stem cell biology. Astrocytes have been shown to induce a neuronal phenotype on adult neural stem cells as a result of cell contact and secreted factors (Song *et al.*, 2002). Microglia can produce neurotrophins, cytokines, and chemokines, acting directly on the neurogenic niches to control precursor cell proliferation, migration. and differentiation (Aarum *et al.*, 2003; Walton *et al.*, 2006; Das and Basu, 2008). Our results show the expression and function of IL-15 in NSCs of the SVZ and in migrating neuroblasts, complementing the previously described expression of the cytokine in astrocytes (Gomez-Nicola *et al.*, 2008a). However, IL-15 is up-regulated on inflammation, to be produced in activated microglial and astroglial cells (Gomez-Nicola *et al.*, 2008a, 2008b), which could be regulating the neurogenic niches both directly and indirectly, through the induction of diffusible factors, growth factors, or proinflammatory cytokines, known products of IL-15–mediated activation (Gomez-Nicola *et al.*, 2010c). The role of cytokines in neurogenesis is still controversial. Several works report that proinflammatory cytokines produced after lipopolysaccharide (LPS)-induced inflammation are detrimental for neurogenesis, through production of TNF-α or IL-6 (Ekdahl *et al.*, 2003; Monje *et al.*, 2003). However, production of anti-inflammatory cytokines like IL-4 or low interferon-γ is associated with the support of neurogenesis (Butovsky *et al.*, 2006). TNF-α has been reported to have both negative and positive actions on neurogenesis. When it signals through its TNFR1 receptor it strongly inhibits neurogenesis, whereas its signaling through TNFR2 is supportive of NSC survival and proliferation (Iosif *et al.*, 2006, 2008). Cytokine IL-6, ciliary neurotrophic factor (CNTF), and leukemia inhibitory factor (LIF) signaling through the gp130 common receptor has been postulated as one important mechanism for regulation of neurogenesis (Carpentier and Palmer, 2009). CNTF and LIF promote NSC self-renewal and astrocyte differentiation (Shimazaki *et al.*, 2001; Taga and Fukuda, 2005). This shift to astrocyte differentiation is also induced by IL-6 in cultured NSCs, reducing production of neurons (Monje *et al.*, 2003; Nakanishi *et al.*, 2007). Other proinflammatory cytokines, like IL-1β, show proneurogenic or antineurogenic actions depending on whether they are expressed basally or pathologically, respectively (Goshen *et al.*, 2008; Koo and Duman, 2008; Spulber *et al.*, 2008). Our results support the hypothesis of the proneurogenic effect of proinflammatory cytokines because basal expression of IL-15 maintains the normal rate of neurogenesis, as evidenced by the experiments with IL-15 knockout mice. When IL-15 is not expressed, the pool of neuroblasts is reduced along the SVZ-RMS axis and recovers after restimulation with recombinant IL-15, never exceeding the wild-type response under this proinflammatory stimulation. Moreover, the evidence of the expression of IL-15Rα within the SVZ points to an autocrine mechanism of action of IL-15. Our previous work on IL-15 biology described the relevant role of the cytokine during the development of neuroinflammation (Gomez-Nicola *et al.*, 2006, 2008a, 2008b, 2010b, 2010c). However, the role of IL-15 in neurogenesis during pathological states and in the cross-talk between glial cells and NSCs remains to be studied, which could be a relevant molecular link during the development of neuroinflammation.

The molecular pathways implicated in the function of IL-15 on NSCs are keys to fully understanding the neurogenic scene. In microglia, IL-15 stimulation activates both ERK and p38 MAPK pathways (Gomez-Nicola *et al.*, 2010c), as previously observed for neutrophils, T, NK, or chronic lymphocytic leukemia B cells (Adunyah *et al.*, 1997; Gadina *et al.*, 2000; de Totero *et al.*, 2008). The IL-15

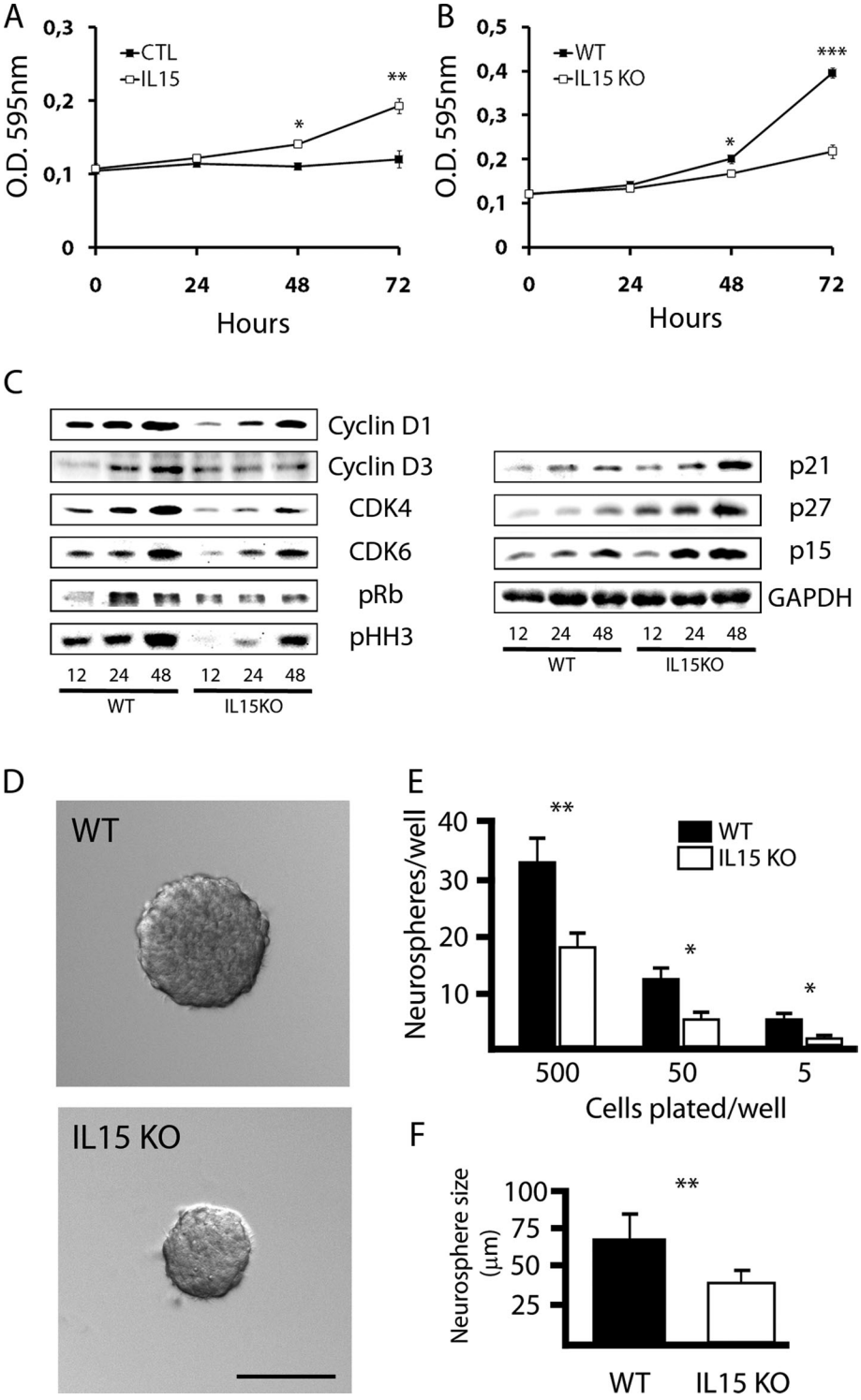


FIGURE 6: IL-15 regulates proliferation and self-renewal of NSCs. (A) Effect of IL-15 on the proliferation of neurospheres, evaluated by the MTT assay. Cells were cultured in incomplete medium (CTL) or incomplete medium supplemented with IL-15 (5 ng/ml) for 24, 48, or 72 h. Data are expressed as mean ± SEM of optical density (OD) 595 nm. (B) Effect of IL-15 deficiency on the proliferation of neurospheres, evaluated by the MTT assay. WT or IL-15 knockout cells were cultured in complete medium for 24, 48, or 72 h. Data are expressed as mean ± SEM of OD 595 nm. (C) Western blotting analysis of the expression of the cell cycle regulators cyclin D1, cyclin D3, CDK4, CDK6, phospho Rb (pRb), phospho histone H3 (pHH3), p21, p27, and p15, using GAPDH as housekeeping gene. WT or IL-15 knockout (KO) neurospheres were cultured for 12, 24, or 48 h in complete medium to further analyze protein expression. (D) Phase contrast analysis of neurosphere size after a self-renewal assay. WT (black bars) and IL-15 knockout (white bars) cells were cultured in complete medium for 7 d to quantify the number of individual cells able to generate a neurosphere (E) and the size of the generated neurospheres (F). (E) Data are expressed as mean ± SEM of the number of neurospheres/well when 5, 50 or 500 cells/well were initially plated. (F) Data are expressed as mean ± SEM of the neurosphere diameter (μm). Scale bar in D, 50 μm. Statistical differences of CTL vs. IL-15 (A), WT vs. IL15 knockout (B, E, F): *$p < 0.05$, **$p < 0.01$, ***$p < 0.001$. Data were analyzed with an ANOVA and a post hoc Tukey test.

receptor system exerts its activities through the activation of the JAK/STAT pathway, preferentially activating JAK1 and STAT3/5 (Hanisch *et al.*, 1997). Moreover, the recruitment of diverse enzymes or cytoplasmic adaptor molecules, like p85, PI3K, Shc, Grb2/Sos, Ras, or Raf, can connect IL-15 signaling with the ERK1/2 and p38 MAPKs (Theze *et al.*, 1996). When IL-15 signals through the IL-2Rb subunit of its receptor it can activate the Shc adaptor molecule and the subsequent activation of the MAPK signaling cascade, with direct effects on both cell survival and proliferation (Ravichandran *et al.*, 1996; Lord *et al.*, 1998; de Totero *et al.*, 2008). Our results show that IL-15 deficiency leads to a defective activation of both the JAK/STAT and the ERK MAPK pathways in adult cultured NSCs. We also show that this defective activation causes a down-regulation of the promoters of the cell cycle (cyclins D1–D3 and CDKs 4–6) with a parallel increase in the levels of the inhibitors (p15, p21, and p27), leading to defective phosphorylation of Rb and pHH3 and to a decrease in the proliferative and self-renewal capacity of the NSCs. The link between MAPK activation and neurogenesis has been described in several works, showing defective neurogenesis on inhibition of MEK1 or ERK2 (Menard *et al.*, 2002; Imamura *et al.*, 2008; Samuels *et al.*, 2008). Although the JAK/STAT pathway was described as a relevant signaling pathway for the determination of the astrocytic differentiation of NSCs (Bonni *et al.*, 1997; Rajan and McKay, 1998), recent reports also point to a direct regulation of neurogenesis (Gu *et al.*, 2005; Ng *et al.*, 2006). Both signaling pathways can also show interconnecting links, regulating NSC proliferation, differentiation, and survival (Kholodenko, 2007). Thus the action of IL-15 in these pathways can be responsible for the maintenance of NSC self-renewal and proliferation in the SVZ, also contributing to the regulation of neurogenesis during neuropathological states.

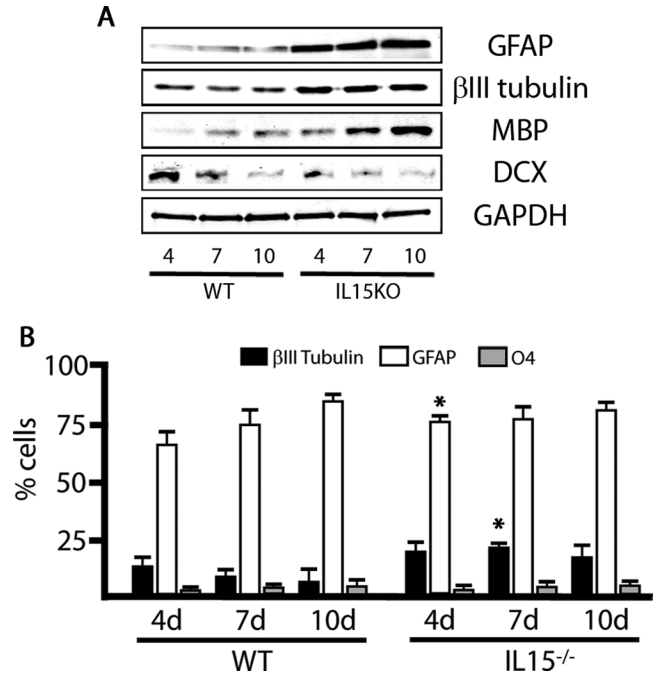


FIGURE 7: IL-15 regulates neurosphere differentiation state. (A) Western blotting analysis of the expression of markers of astrocytes (GFAP), neurons (βIII tubulin), oligodendrocytes (MBP), and neural progenitor cells (DCX) in WT and IL-15 knockout NSCs cultured in differentiating conditions (2% FBS; poly-L-lysine) for 4, 7, or 10 d. (B) Immunocytochemical analysis of the cellular proportions during differentiation of NSCs of WT or IL-15 KO cells. Cells were cultured in differentiating medium (2% FBS; poly-L-lysine) for 4, 7, or 10 d and analyzed for the percent of neurons (βIII tubulin+; black bars), astrocytes (GFAP+; white bars), or oligodendrocytes (O4+; gray bars), expressing data as mean ± SEM of positive cells. Statistical differences of WT vs. IL-15−/−: *$p < 0.05$. Data were analyzed with an ANOVA and a post hoc Tukey test.

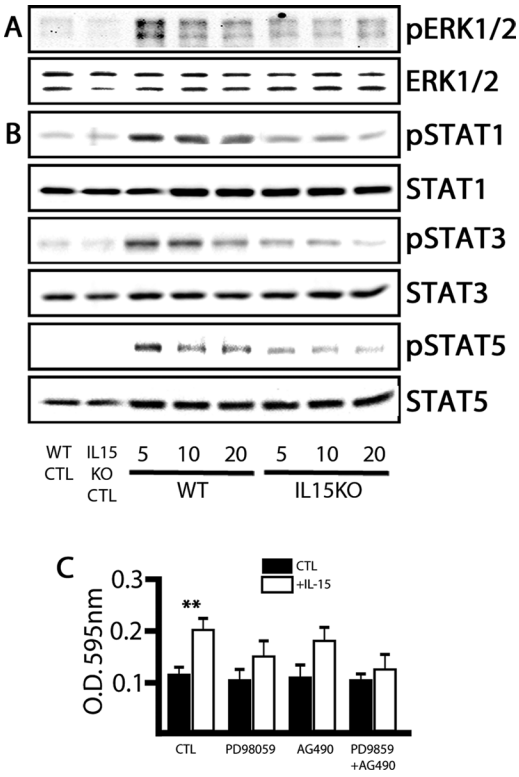


FIGURE 8: IL-15 regulates the activation of the ERK and JAK/STAT signaling pathways. (A) Western blotting analysis of the activation of the ERK MAPK pathway. The activation of ERK1 and ERK2 is represented by the phosphorylation degree (up; pERK1/2) in relation to the total protein (down; ERK1/2). (B) Western blotting analysis of the activation of the JAK/STAT pathway. The activation of STAT1, STAT3, and STAT5 is represented by the phosphorylation degree (pSTAT1, pSTAT3, pSTAT5) in relation to the total protein (STAT1, STAT3, STAT5). WT and IL-15 KO neurospheres were treated with complete medium for 5, 10, and 20 min, using cells treated with incomplete medium as controls (WT CTL, IL-15 KO CTL). (C) Effect of the inhibition of IL-15 signaling on the proliferation of neurospheres was evaluated by the MTT assay. In the control conditions, cells were cultured in incomplete medium (CTL) or incomplete medium supplemented with IL-15 (5 ng/ml) for 72 h. Alternatively, cells were treated with PD98059, AG-490, or the combination. Data are expressed as mean ± SEM of OD 595 nm. Statistical differences of CTL vs. IL-15: **$p < 0.01$. Data were analyzed with an ANOVA and a post hoc Tukey test.

## MATERIALS AND METHODS

### Animals

IL-15−/− (Kennedy *et al.*, 2000) and C57BL/6 mice were originally purchased from Taconic (Germantown, NY) and Harlan Labs (Barcelona, Spain), respectively. Both lines were in-house crossed for colony establishment and maintenance (Cajal Institute, Madrid, Spain). Mice were kept on food and water ad libitum in a 12-h light/dark cycle. Handling of animals was performed in compliance with the guidelines of animal care set by the European Union (86/609/EEC) and the Cajal Institute animal welfare committee.

### Neurosphere cultures

Neurosphere cultures were prepared from the SVZ of adult mice and maintained in complete medium containing Neurobasal (Invitrogen, Carlsbad, CA), 2% B27 supplement (Invitrogen, Carlsbad, CA), 2 mM L-glutamine, penicillin/streptomycin (Sigma-Aldrich, St. Louis, MO), 20 ng/ml of recombinant murine EGF (EGF; Peprotech, Rocky Hill, NJ), and 10 ng/ml of recombinant human basic fibroblast growth factor (bFGF; Peprotech). Proliferation of neurospheres was assessed using the 3-(4,5-dimethyl-thiazol-2-yl) 2,5-diphenyl tetrazolium bromide (MTT) reduction method (n = 6), as previously described (Valle-Argos *et al.*, 2010a). Briefly, dissociated cells from WT or IL-15−/− mice were seeded in 96-well plates ($5 \times 10^3$ cells/well) and incubated in complete medium for different periods of time to further evaluate proliferation by the differential reduction degree of the MTT. Alternatively, WT cells were treated with incomplete medium (complete medium without EGF or FGF) or incomplete medium supplemented with recombinant mouse IL-15 (5 ng/ml; Peprotech) and cultured for 24, 48, or 72 h. Compounds PD98059 and AG490 (Sigma-Aldrich) were used to block MEK or JAK activity. Proliferation was expressed as optical density at 595 nm, referring absorbance values to that of empty wells.

To evaluate the self-renewal capacity of the cultured NSCs, we used a clonal colony-forming assay to measure the proportion of cells that were able to make new neurospheres. Single cell-dissociated cultures of NSCs were plated into 96-well culture plates with 5, 50, or 500 cells per well, and the number of newly formed neurospheres was counted after 7 d. The number of new neurospheres (>20 cells tightly attached to each other) was assessed by light microscopy and represented as number of neurospheres/well. Moreover, newly formed neurospheres after 7 d of the self-renewal assay were photographed under a 10× lens, measuring its size (mean

diameter in micrometers) with the help of ImageJ software (Rasband, 2008).

For differentiation assays dissociated single-cell cultures were plated on poly-L-lysine-coated surfaces ($5 \times 10^4$ cells/mm$^2$) and cultured with complete medium supplemented with 2% FBS for 4, 7, or 10 d.

### Immunohistochemistry

IL-15−/− and WT mice perfusion, tissue processing, and immunohistochemical analysis was performed as previously described (Gomez-Nicola *et al.*, 2008a; Valle-Argos *et al.*, 2010b). The sections were treated successively with 1% methanol/30% $H_2O_2$ and 5% normal donkey serum/0.1% bovine serum albumin (BSA), to block endogenous peroxidase and nonspecific binding, respectively. After repeated rinses with PBS + Tween 20 (PBST; 0.1% vol/vol), they were incubated overnight at 4°C using the following primary antibodies: goat anti–mouse IL-15 (Santa Cruz Biotechnologies, Santa Cruz, CA), goat anti–mouse IL-15Rα (Santa Cruz Biotechnologies), guinea pig anti–mouse doublecortin (Chemicon, Temecula, CA), mouse anti–mouse nestin (Abcam, Cambridge, United Kingdom), and mouse anti–mouse GFAP (Chemicon). After primary antibody incubation, the sections were washed with PBST and incubated with the appropriate biotinylated secondary antibody (Jackson ImmunoResearch, West Grove, PA) or with the appropriate Alexa 488- or 594–conjugated secondary antibody (Molecular Probes, Leiden, Netherlands). For light microscopy, the sections were washed and incubated with Vectastain ABC complex (Vector Laboratories, Burlingame, CA) and visualized using diaminobenzidine precipitation. Sections for light microscopy were mounted with DePeX (BDH, Poole, United Kingdom) and visualized in an Olympus Provis AX70 microscope coupled to an Olympus DP71 image acquisition system. After immunofluorescence labeling, nuclei were visualized by Hoechst staining, and the sections were mounted with glycerol/1,4-diazabicyclo[2.2.2]octane (DABCO) mixture. The sections were visualized on a Leica TCS-SP5 confocal system coupled to a Leica DMI6000CS microscope. Specificity of the primary antibodies was shown in previous work (Gomez-Nicola *et al.*, 2008a, 2008b, 2010c).

### EdU/BrDU labeling

The analysis of neurogenesis in adult IL-15−/− and WT mice was performed after intraperitoneal (IP) injection of BrDU and immunohistochemical analysis (n = 8). BrDU (Sigma-Aldrich) was dissolved in PBS (7.5 mg/ml) and administered in eight doses during 2 d at a dose of 0.1 ml/10 g of mouse weight. BrDU incorporation was evidenced using the general immunohistochemical method with the following modifications. Before the blocking step, sections were treated with two cycles of boiling 10 mM sodium citrate buffer (antigen retrieval) followed by washes and treatment with 2 N HCl (30 min, 37°C, denaturation step). Mouse anti-BrDU (1:2000; Developmental Studies Hybridoma Bank, University of Iowa, Iowa City, IO) was used as primary antibody, using the secondary antibodies as described in the next section.

The study of the effect of IL-15 on neurogenesis using sequential incorporation of EdU and BrdU used the following experimental protocol (Figure 3; n = 5). EdU (Click-iT EdU Imaging Kit; Invitrogen) was administered at t = 0, 10, and 20 h (IP; 7.5 mg/ml in PBS, 0.1 ml/10 g mouse). The animals received, 24 h after the first dose of EdU, a single intraventricular injection of IL-15 (1 μg in 5 μl of PBS; Peprotech) or PBS (vehicle; 5 μl), as previously described (Gomez-Nicola *et al.*, 2008a). Then animals were treated with BrDU at t = 24, 34, and 44 h (IP; 7.5 mg/ml in PBS, 0.1 ml/10 g mouse), to be finally perfused 48 h after the first injection. With this protocol, leaving 4 h between the last EdU and the first BrDU injection and knowing that BrDU is preferentially incorporated to the DNA when compared with EdU, the possible incorporation of EdU after IL-15/PBS injection was avoided. BrDU was evidenced as previously described, and EdU was visualized using the Click-iT reaction coupled to an Alexa Fluor 488 azide following the instructions of the manufacturer (Invitrogen).

Alternatively, an additional group of IL-15−/− or WT mice received an intraventricular injection of IL-15 or PBS only, as previously described, to be perfused after 24 h, for the analysis of the effect of IL-15 on DCX expression by immunohistochemical means (Figure 4).

### Immunocytochemistry

The analysis of IL-15 expression in neurospheres was performed under proliferative conditions (complete medium) by plating the neurospheres on glass coverslips (Menzer Glaser, Braunschweig, Germany) to permit attachment for 10 min before fixation. The analysis of neurosphere differentiation was performed on cells growing under differentiation conditions (complete medium supplemented with 2% FBS; 4, 7, or 10 d) over glass coverslips coated with poly-L-lysine. Immunofluorescence staining was performed as previously described (Gomez-Nicola *et al.*, 2008a). The cells were incubated with goat anti-mouse IL-15 (Santa Cruz Biotechnologies), guinea pig anti–mouse DCX (Chemicon), mouse anti–mouse nestin (Abcam), mouse anti–mouse GFAP (Chemicon), rabbit anti–mouse MBP (Abcam), mouse anti–mouse βIII tubulin (Sigma-Aldrich), or mouse anti–mouse O4 (Chemicon, Temecula, CA). Primary antibodies were visualized with the appropriate Alexa-conjugated secondary antibodies (Molecular Probes). Cells were additionally stained with Hoechst dye to visualize their nuclei. Slides were mounted with glycerol/PBS, 2/1 (vol/vol) with DABCO (Sigma-Aldrich) at a concentration of 25 mg/ml and photographed with a Leica TCS-SP5 digital confocal system coupled to a Leica DMI6000CS microscope. Slides incubated without primary antibody were used as negative controls. Specificity of the primary antibodies was established previously (Gomez-Nicola *et al.*, 2008a, 2010c).

### Western blotting

Processing of neurospheres cell samples and analysis of protein expression were performed as previously described (Gomez-Nicola *et al.*, 2008b; Valle-Argos *et al.*, 2011). After incubation with the different treatments at the specific time points, cells were processed and samples (20 μg protein/lane) were electrophoresed and transferred to nitrocellulose membranes (Whatman GmbH, Dassel, Germany). After blocking of nonspecific binding, the blots were incubated with the following primary antibodies: rabbit anti–phospho histone H3 (Ser10; Millipore, Billerica, MA), mouse anti-p21waf1/cip1 (Cell Signaling), rabbit anti-p27kip1 (Cell Signaling), rabbit anti-p15 (Cell Signaling), mouse anti-cyclin D1 (Cell Signaling), mouse anti–cyclin D3 (Cell Signaling), mouse anti-CDK4 (Cell Signaling), mouse anti-CDK6 (Cell Signaling), rabbit anti–phospho Rb (Cell Signaling), mouse anti–phospho p42/44 MAPK (Sigma-Aldrich), rabbit anti–p42/44 MAPK (Sigma-Aldrich), rabbit anti-STAT1 (Cell Signaling), rabbit anti-STAT3 (Cell Signaling), rabbit anti-STAT5 (Cell Signaling), rabbit anti–phospho STAT1 (Cell Signaling), rabbit anti–phospho STAT3 (Cell Signaling), rabbit anti–phospho STAT5 (Cell Signaling), mouse anti-GFAP (Chemicon), mouse anti–βIII tubulin (Sigma-Aldrich), rabbit anti-MBP (Abcam), and guinea pig anti-DCX (Chemicon), using mouse anti–glyceraldehyde phosphate dehydrogenase (Chemicon) as loading control. Blots were incubated with the specific horseradish peroxidase–conjugated secondary antibody

(Jackson ImmunoResearch), and then protein bands were detected using SuperSignal West Pico Chemiluminescent Substrate (Pierce Biotechnology, Rockford, IL).

### Reverse transcriptase-PCR

To analyze mRNA expression by reverse transcriptase-PCR (RT-PCR) (Gomez-Nicola et al., 2006), NSC RNA was extracted with TRIzol reagent (Invitrogen), determining mRNA expression (n = 4) with the Titan One-Tube RT-PCR System commercial kit (Roche Diagnostics, Mannheim, Germany). The reaction mixture was prepared by adding 500 ng of previously quantified RNA. The primers for IL-15 (NM_013129; left 5′ tctcttcttcatcctccccttg 3′, right 5′ ggttttctcctccagctcctcac 3′) were synthesized (Sigma-Genosys, The Woodlands, TX). Glyceraldehyde-3-phosphate dehydrogenase (NM_017008; left 5′ tgccactcagaagactgtggatg 3′, right 5′ ccagcatcaaaggtggaagaatg 3′) was used as housekeeping gene for expression control, and a reaction mixture without RNA sample was used as an internal control in every reaction. RT-PCR products were UV visualized and photographed.

### Quantification and image analysis

To quantify neurogenesis in the SVZ, BrdU+ cells from the lateral wall of the lateral ventricle were counted; data are represented as number of BrdU+ cells/mm$^2$ (n = 6 sections per animal, eight animals per group). To quantify proliferation in the RMS, we counted BrdU+ cells within the area in which they were contained; data are represented as number of BrdU+ cells/mm$^2$ (n = 4 sections per animal, eight animals per group). EdU+ or BrDU+ cells were counted in the SVZ or the RMS in immunofluorescent images obtained by confocal microscopy and as delimited by Hoechst staining. After obtaining the individual number of BrDU or EdU +cells/mm$^2$, data were expressed as BrDU/EdU ratio (n = 5 sections per animal, five animals per group). Sections from similar anatomical levels of the RMS (from bregma +1.7 to +2.3) or the SVZ (from bregma +0.1 to +0.9) were processed at the same time for each type of staining. Countings were performed in double blind by two independent investigators.

The expression of DCX and GFAP was quantified with the help of an image analysis system (AIS; Imaging Research, Linton, United Kingdom), using a 10× lens, as previously described (Gomez-Nicola et al., 2008a, 2010b). The data are presented as percent proportional area (epitope-positive area/scan area). The proportional stained area for DCX or GFAP was determined in the SVZ and the RMS (n = 5 sections per animal, five animals per group).

Quantification of the number of secondary neurospheres in the self-renewal experiments was performed in three different 10× fields/well (n = 6 wells/treatment).

For the differentiation assays, GFAP+, βIII tubulin+, or O4+ cells were counted in five different 20× fields/well (n = 4 wells/treatment). Data are expressed as percent of immunopositive cells related to the total number of cells measured by the number of Hoechst+ nuclei.

All quantifications were performed with the help of ImageJ image analysis software (Rasband, 2008).

### Statistical analysis

Data are expressed as mean ± SEM and analyzed with the STATISTICA 6.0 software package from StatSoft (Tulsa, OK). For all data sets, normality and homoscedasticity assumptions were reached, validating the application of the one-way analysis of variance, followed by the Tukey post hoc test for multiple comparisons. Differences were considered significant for $p < 0.05$.

## ACKNOWLEDGMENTS

This work was supported by grants from the Fundación Inocente-Inocente, the Fundación Hospital Nacional de Parapléjicos para la Investigación y la Integración, and the Spanish Minister of Science and Innovation (MINCIIN; SAF 2006–11224). B.V.-A. was funded by an FPU fellowship of the Spanish Department of Education (MEC). We thank Jesus Díaz Tobarra for technical help.

## REFERENCES

Aarum J, Sandberg K, Haeberlein SL, Persson MA (2003). Migration and differentiation of neural precursor cells can be directed by microglia. Proc Natl Acad Sci USA 100, 15983–15988.

Adunyah SE, Wheeler BJ, Cooper RS (1997). Evidence for the involvement of LCK and MAP kinase (ERK-1) in the signal transduction mechanism of interleukin-15. Biochem Biophys Res Commun 232, 754–758.

Alvarez-Buylla A, Garcia-Verdugo JM, Tramontin AD (2001). A unified hypothesis on the lineage of neural stem cells. Nat Rev Neurosci 2, 287–293.

Bauer S (2009). Cytokine control of adult neural stem cells. Ann NY Acad Sci 1153, 48–56.

Beck RD Jr, Wasserfall C, Ha GK, Cushman JD, Huang Z, Atkinson MA, Petitto JM (2005). Changes in hippocampal IL-15, related cytokines, and neurogenesis in IL-2 deficient mice. Brain Res 1041, 223–230.

Benson DM Jr, Yu J, Becknell B, Wei M, Freud AG, Ferketich AK, Trotta R, Perrotti D, Briesewitz R, Caligiuri MA (2009). Stem cell factor and interleukin-2/15 combine to enhance MAPK-mediated proliferation of human natural killer cells. Blood 113, 2706–2714.

Bonni A, Sun Y, Nadal-Vicens M, Bhatt A, Frank DA, Rozovsky I, Stahl N, Yancopoulos GD, Greenberg ME (1997). Regulation of gliogenesis in the central nervous system by the JAK-STAT signaling pathway. Science 278, 477–483.

Budagian V, Bulanova E, Paus R, Bulfone-Paus S (2006). IL-15/IL-15 receptor biology: a guided tour through an expanding universe. Cytokine Growth Factor Rev 17, 259–280.

Butovsky O, Ziv Y, Schwartz A, Landa G, Talpalar AE, Pluchino S, Martino G, Schwartz M (2006). Microglia activated by IL-4 or IFN-gamma differentially induce neurogenesis and oligodendrogenesis from adult stem/progenitor cells. Mol Cell Neurosci 31, 149–160.

Carpentier PA, Palmer TD (2009). Immune influence on adult neural stem cell regulation and function. Neuron 64, 79–92.

Das S, Basu A (2008). Inflammation: a new candidate in modulating adult neurogenesis. J Neurosci Res 86, 1199–1208.

de Totero D, Meazza R, Capaia M, Fabbi M, Azzarone B, Balleari E, Gobbi M, Cutrona G, Ferrarini M, Ferrini S (2008). The opposite effects of IL-15 and IL-21 on CLL B cells correlate with differential activation of the JAK/STAT and ERK1/2 pathways. Blood 111, 517–524.

Doetsch F, Caille I, Lim DA, Garcia-Verdugo JM, Alvarez-Buylla A (1999). Subventricular zone astrocytes are neural stem cells in the adult mammalian brain. Cell 97, 703–716.

Ekdahl CT, Claasen JH, Bonde S, Kokaia Z, Lindvall O (2003). Inflammation is detrimental for neurogenesis in adult brain. Proc Natl Acad Sci USA 100, 13632–13637.

Ekdahl CT, Kokaia Z, Lindvall O (2009). Brain inflammation and adult neurogenesis: the dual role of microglia. Neuroscience 158, 1021–1029.

Fehniger TA, Caligiuri MA (2001). Interleukin 15: biology and relevance to human disease. Blood 97, 14–32.

Gadina M, Sudarshan C, Visconti R, Zhou YJ, Gu H, Neel BG, O'Shea JJ (2000). The docking molecule gab2 is induced by lymphocyte activation and is involved in signaling by interleukin-2 and interleukin-15 but not other common gamma chain-using cytokines. J Biol Chem 275, 26959–26966.

Giron-Michel J *et al.* (2003). Differential STAT3, STAT5, and NF-kappaB activation in human hematopoietic progenitors by endogenous interleukin-15: implications in the expression of functional molecules. Blood 102, 109–117.

Gomez-Nicola D, Doncel-Perez E, Nieto-Sampedro M (2006). Regulation by GD3 of the proinflammatory response of microglia mediated by interleukin-15. J Neurosci Res 83, 754–762.

Gomez-Nicola D, Pallas-Bazarra N, Valle-Argos B, Nieto-Sampedro M (2010a). CCR7 is expressed in astrocytes and upregulated after an inflammatory injury. J Neuroimmunol 227, 87–92.

Gomez-Nicola D, Spagnolo A, Guaza C, Nieto-Sampedro M (2010b). Aggravated experimental autoimmune encephalomyelitis in IL-15 knockout mice. Exp Neurol 222, 235–242.

Gomez-Nicola D, Valle-Argos B, Nieto-Sampedro M (2010c). Blockade of IL-15 activity inhibits microglial activation through the NFkappaB, p38, and ERK1/2 pathways, reducing cytokine and chemokine release. Glia 58, 264–276.

Gomez-Nicola D, Valle-Argos B, Pita-Thomas DW, Nieto-Sampedro M (2008a). Interleukin 15 expression in the CNS: blockade of its activity prevents glial activation after an inflammatory injury. Glia 56, 494–505.

Gomez-Nicola D, Valle-Argos B, Suardiaz M, Taylor JS, Nieto-Sampedro M (2008b). Role of IL-15 in spinal cord and sciatic nerve after chronic constriction injury: regulation of macrophage and T-cell infiltration. J Neurochem 107, 1741–1752.

Goshen I, Kreisel T, Ben-Menachem-Zidon O, Licht T, Weidenfeld J, Ben-Hur T, Yirmiya R (2008). Brain interleukin-1 mediates chronic stress-induced depression in mice via adrenocortical activation and hippocampal neurogenesis suppression. Mol Psychiatry 13, 717–728.

Gu F, Hata R, Ma YJ, Tanaka J, Mitsuda N, Kumon Y, Hanakawa Y, Hashimoto K, Nakajima K, Sakanaka M (2005). Suppression of Stat3 promotes neurogenesis in cultured neural stem cells. J Neurosci Res 81, 163–171.

Hanisch UK, Lyons SA, Prinz M, Nolte C, Weber JR, Kettenmann H, Kirchhoff F (1997). Mouse brain microglia express interleukin-15 and its multimeric receptor complex functionally coupled to Janus kinase activity. J Biol Chem 272, 28853–28860.

He Y *et al*. (2010). Interleukin-15 receptor is essential to facilitate GABA transmission and hippocampal-dependent memory. J Neurosci 30, 4725–4734.

Huang YS *et al*. (2009). Effects of interleukin-15 on neuronal differentiation of neural stem cells. Brain Res 1304, 38–48.

Huang Z, Ha GK, Petitto JM (2007). IL-15 and IL-15R alpha gene deletion: effects on T lymphocyte trafficking and the microglial and neuronal responses to facial nerve axotomy. Neurosci Lett 417, 160–164.

Imamura O, Satoh Y, Endo S, Takishima K (2008). Analysis of extracellular signal-regulated kinase 2 function in neural stem/progenitor cells via nervous system–specific gene disruption. Stem Cells 26, 3247–3256.

Iosif RE, Ekdahl CT, Ahlenius H, Pronk CJ, Bonde S, Kokaia Z, Jacobsen SE, Lindvall O (2006). Tumor necrosis factor receptor 1 is a negative regulator of progenitor proliferation in adult hippocampal neurogenesis. J Neurosci 26, 9703–9712.

Iosif RE, Ahlenius H, Ekdahl CT, Darsalia V, Thored P, Jovinge S, Kokaia Z, Lindvall O (2008). Suppression of stroke-induced progenitor proliferation in adult subventricular zone by tumor necrosis factor receptor 1. J Cereb Blood Flow Metab 28, 1574–1587.

Kennedy MK *et al*. (2000). Reversible defects in natural killer and memory CD8 T cell lineages in interleukin 15–deficient mice. J Exp Med 191, 771–780.

Kholodenko BN (2007). Untangling the signalling wires. Nat Cell Biol 9, 247–249.

Koo JW, Duman RS (2008). IL-1beta is an essential mediator of the antineurogenic and anhedonic effects of stress. Proc Natl Acad Sci USA 105, 751–756.

Li L, Walker TL, Zhang Y, Mackay EW, Bartlett PF (2010). Endogenous interferon gamma directly regulates neural precursors in the non-inflammatory brain. J Neurosci 30, 9038–9050.

Lord JD, McIntosh BC, Greenberg PD, Nelson BH (1998). The IL-2 receptor promotes proliferation, bcl-2 and bcl-x induction, but not cell viability through the adapter molecule Shc. J Immunol 161, 4627–4633.

Menard C *et al*. (2002). An essential role for a MEK-C/EBP pathway during growth factor-regulated cortical neurogenesis. Neuron 36, 597–610.

Monje ML, Toda H, Palmer TD (2003). Inflammatory blockade restores adult hippocampal neurogenesis. Science 302, 1760–1765.

Nakanishi M, Niidome T, Matsuda S, Akaike A, Kihara T, Sugimoto H (2007). Microglia-derived interleukin-6 and leukaemia inhibitory factor promote astrocytic differentiation of neural stem/progenitor cells. Eur J Neurosci 25, 649–658.

Ng DC, Lin BH, Lim CP, Huang G, Zhang T, Poli V, Cao X (2006). Stat3 regulates microtubules by antagonizing the depolymerization activity of stathmin. J Cell Biol 172, 245–257.

Rajan P, McKay RD (1998). Multiple routes to astrocytic differentiation in the CNS. J Neurosci 18, 3620–3629.

Rasband W (2008). ImageJ. Image Processing and Analysis in Java, Version 1.38x, National Institutes of Health, Bethesda, MD. Available from http://rsb.info.nih.gov/ij/.

Ravichandran KS, Igras V, Shoelson SE, Fesik SW, Burakoff SJ (1996). Evidence for a role for the phosphotyrosine-binding domain of Shc in interleukin 2 signaling. Proc Natl Acad Sci USA 93, 5275–5280.

Samuels IS, Karlo JC, Faruzzi AN, Pickering K, Herrup K, Sweatt JD, Saitta SC, Landreth GE (2008). Deletion of ERK2 mitogen-activated protein kinase identifies its key roles in cortical neurogenesis and cognitive function. J Neurosci 28, 6983–6995.

Shimazaki T, Shingo T, Weiss S (2001). The ciliary neurotrophic factor/leukemia inhibitory factor/gp130 receptor complex operates in the maintenance of mammalian forebrain neural stem cells. J Neurosci 21, 7642–7653.

Song H, Stevens CF, Gage FH (2002). Astroglia induce neurogenesis from adult neural stem cells. Nature 417, 39–44.

Spulber S, Oprica M, Bartfai T, Winblad B, Schultzberg M (2008). Blunted neurogenesis and gliosis due to transgenic overexpression of human soluble IL-1ra in the mouse. Eur J Neurosci 27, 549–558.

Taga T, Fukuda S (2005). Role of IL-6 in the neural stem cell differentiation. Clin Rev Allergy Immunol 28, 249–256.

Theze J, Alzari PM, Bertoglio J (1996). Interleukin 2 and its receptors: recent advances and new immunological functions. Immunol Today 17, 481–486.

Umehara T, Udagawa J, Takamura K, Kimura M, Ishimitsu R, Kiyono H, Kawauchi H, Otani H (2009). Role of interleukin-15 in the development of mouse olfactory nerve. Congenit Anom (Kyoto) 49, 253–257.

Valle-Argos B, Gomez-Nicola D, Nieto-Sampedro M (2010a). Synthesis and characterization of neurostatin-related compounds with high inhibitory activity of glioma growth. Eur J Med Chem 45, 2034–2043.

Valle-Argos B, Gomez-Nicola D, Nieto-Sampedro M (2010b). Glioma growth inhibition by neurostatin and O-But GD1b. Neuro Oncol 12, 1135–1146.

Valle-Argos B, Gomez-Nicola D, Nieto-Sampedro M (2011). Neurostatin blocks glioma cell cycle progression by inhibiting EGFR activation. Mol Cell Neurosci 46, 89–100.

Vallieres L, Campbell IL, Gage FH, Sawchenko PE (2002). Reduced hippocampal neurogenesis in adult transgenic mice with chronic astrocytic production of interleukin-6. J Neurosci 22, 486–492.

Walton NM, Sutter BM, Laywell ED, Levkoff LH, Kearns SM, Marshall GP, Scheffler B, Steindler DA (2006). Microglia instruct subventricular zone neurogenesis. Glia 54, 815–825.

Wu X, He Y, Hsuchou H, Kastin AJ, Rood JC, Pan W (2010). Essential role of interleukin-15 receptor in normal anxiety behavior. Brain Behav Immun 24, 1340–1346.

Wu X, Hsuchou H, Kastin AJ, He Y, Khan RS, Stone KP, Cash MS, Pan W (2011). Interleukin-15 affects serotonin system and exerts antidepressive effects through IL15Rα receptor. Psychoneuroendocrinology 36, 266–278